Optimal Real-time Trajectory Planning for a Fixed Wing Vehicle in 3D Dynamic Environment

Wenhao Luo, Jun Peng*, *Member, IEEE,* and Jing Wang, *Senior Member, IEEE*

Abstract— In this paper, an on-line motion planner is described to determine an optimal and collision-free trajectory for fixed wing vehicles moving in a 3D space populated with static hills and movable obstacles. The proposed method is mainly based on the polynomial parameterization of trajectories, which is beneficial to explicitly consider the kinematic constraints and the geometric constraints resulted from obstacles. The near shortest trajectory is chosen by optimizing a performance index with respect to path length. By design, the optimal trajectory planning could boil down to solve a constrained optimization problem with respect to three adjustable path parameters, which can be well handled in a transformed 3D parameter space. The resultant trajectories satisfy all boundary conditions and the analytically derived control inputs are always smooth to be implemented on real-time planning. Computer simulation results verify the effectiveness of the proposed approach.

I. INTRODUCTION

The motion planning problem is a key issue for vehicles in the discussion of autonomy and navigation, which should take into consideration of kinematic constraints, collision avoidance criterion, optimization on energy or path length, etc [1]. For a flying vehicle [2] operating in 3D cluttered dynamic space, we may hope to simultaneously consider problems of feasibility and optimality, and ensure the computational efficiency for on-line planning.

The search-based algorithms such as rapidly exploring random trees(RRT/RRT*) [3][4] could be applied in 3D planning. A random sampling search is conducted that fast explores the C-space with a sampling scheme governed by collision detection module, and embeds kinematic and kinodynamic constraints of the robot. Such method can also be modified to handle the 3D flying vehicle kinematic model [5]. Another search algorithm based on A* is proposed in [6] to overcome typical shortcomings of spurious turns existent in other grid-based approaches. In local dynamic environment, however, these methods may not be able to handle moving obstacles while guaranteeing the optimality.

In order to handle the dynamic planning more efficiently, an analytic method is pioneered in [7] and further improved in [8]. In [9] energy-optimal and path length-optimal

W. Luo is with the Department of Automation, Shanghai Jiao Tong University, and Key Laboratory of System Control And Information Processing, Ministry of Education of China, Shanghai, 200240, China (e-mail:whluo@sjtu.edu.cn).

J. Peng is with the School of Information Science and Engineering, Central South University, and Hunan Engineering Laboratory for Advanced Control and Intelligent Automation, Changsha, 410083, China (e-mail: pengj@csu.edu.cn).

Corresponding Author: J. Peng, pengj@csu.edu.cn

J. Wang is with the Computer Engineering Program, Bethune-Cookman University, Daytona Beach, FL 32114 USA (e-mail: wangj@cookman.edu).

solutions are addressed in closed form. [10][11] modify canonical analytic solution for the purpose of 3D planning. However, lack of consideration on higher dimensional states makes the reference control inputs discrete and nonsmooth. Nonetheless, the idea of parametric method is ideal to fast compute feasible paths for real-time planning.

In this paper, the problem of on-line motion planning for flying vehicle is addressed with three steps. First, the parametric trajectory model determined by three specific parameters is developed based on the boundary conditions and differential flatness. Second, the performance index and its optimal solution are explicitly given, and the geometric constraints due to obstacles are transferred into a set of constraint equations with respect to those parameters, which then recasts the trajectory generation problem as a constrained optimization problem. Finally, such a problem could be redefined in a parameter space that unifies the discussion of collision-avoidance criterion and performance index. The suboptimal solution can thereby be obtained and periodically updated to incorporate dynamic environment. Such an approach provides a good solution to fast compute feasible paths in local dynamic unknown surroundings, which may also be exploited by algorithms such as RRT to achieve global planning in complex environment.

This paper is organized as follows. Section II introduces the vehicle model, environment model and the optimal motion planning problem. In section III, optimal solution and collision avoidance criterion amidst obstacles will be analytically considered and combined to compute desired optimal path in the parameter space. Simulation results are shown and discussed in section IV to prove the effectiveness of the approach. In section V, conclusions are drawn.

II. PROBLEM STATEMENT

For a fixed wing flying vehicle, there are generally three forces [2]. They are the thrust force T from the engine along the vehicle fuselage, the aerodynamic lift force L normal to the direction of velocity v and the lift-drag plane, and the aerodynamic drag force D against the direction of velocity v. The flying vehicle and the relationship of the forces in the coordinate systems are shown in Fig.1.

As described in [2], here the point-mass M is the origin of two coordinate systems: the local-horizon system $x' - y' - z'$ and the wind-axis system $x_1 - y_1 - z_1$. The two rotations from $x' - y' - z'$ to $x_1 - y_1 - z_1$ are directional angle ψ (about x') and flight-path angle γ (about negative z_1). In the global coordinate system, the location of M that represents the vehicle's position is expressed by Cartesian coordinates

Fig. 1. Fixed wing vehicle model, coordinate systems and forces

Fig. 2. Fixed wing vehicle moving in a dynamic environment.

(x, y, h)(to unify the symbol, h is replaced by z in the rest parts). The geometric model of flying vehicle is its smallest circumference with radius R. The angle ε, ψ, γ and σ(the angle between the vector L and the vertical plane) are referred to as the attack angle, yaw angle, pitch angle and roll angle respectively.

For the pilot, the control inputs of the flying vehicle are forces F_T (throttle), F_N(stick pull-push), and the banking angle σ(stick left-right). The two resultant forces F_T and F_N can be given by

$$F_T = T cos\varepsilon - D, \qquad F_N = T sin\varepsilon + L \qquad (1)$$

F_T is along the velocity vector that speeds up the vehicle. F_N can be decomposed into a component $F_N cos\sigma$ in the vertical plane and orthogonal to v, which directly affects vehicle pitch motion, and the other component $F_N sin\sigma$ orthogonal to the vertical, which affects vehicle yaw motion. The kinematics and motion equations of a flying vehicle are as follows.

$$\dot{x} = v cos\gamma cos\psi, \quad \dot{y} = v cos\gamma sin\psi, \quad \dot{z} = v sin\gamma \quad (2)$$

$$\dot{v} = \frac{F_T}{M} - g sin\gamma, \; \dot{\gamma} = \frac{F_N cos\sigma}{Mv} - \frac{g cos\gamma}{v}, \; \dot{\psi} = \frac{F_N sin\sigma}{Mv cos\gamma} \quad (3)$$

where g is the local gravitational acceleration. M is the vehicle point mass.

A desired trajectory planner should drive the flying vehicle from initial condition $q^0 = (x_0, y_0, z_0, v_0, \psi_0, \gamma_0, \sigma_0)^T$ at time t_0 to terminal condition $q^f = (x_f, y_f, z_f, v_f, \psi_f, \gamma_f, \sigma_f)^T$ at time t_f. As shown in Fig.2, the surrounding environment may contain stationary hill-like obstacles and movable ones, i.e. other vehicles or missiles. Considering the kinematic constraints of the flying vehicle and geometric constraints due to obstacles, the problem can be formulated as follows:

$$\begin{aligned} \min &J(q, \dot{q}) \\ s.t. \quad &q(t_0) = q^0 \\ &q(t_f) = q^f \\ &M(q, \dot{q}) = 0 \\ &F(x(t), y(t), z(t)) \geq 0 \end{aligned} \qquad (4)$$

where $J(q, \dot{q})$ is a performance index(PI) related to path length. $M(q, \dot{q})$ indicates the kinematic constraints of the flying vehicle. $F(x(t), y(t), z(t))$ denotes geometric constraints obtained from collision avoidance criteria.
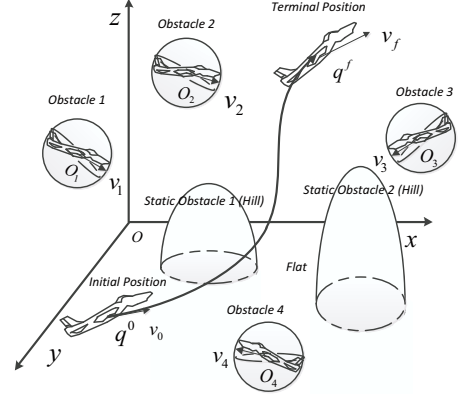
III. ON-LINE OPTIMAL TRAJECTORY GENERATION FOR FIXED WING VEHICLE

A. Trajectory Model and Control Inputs

Inspired by the polynomial parameterization approach in [7], we formulate the trajectory model by three independent six-order polynomials with respect to time in order to better approximate feasible paths and avoid control discontinuity problem that exists in [11]. Then a family of trajectories can be given as follows.

$$x(t) = \vec{c} \, f(t), \quad y(t) = \vec{d} \, f(t), \quad z(t) = \vec{e} \, f(t) \quad (5)$$

where $\vec{c} = [c_0 \, c_1 \, c_2 \, \dots \, c_6]$, $\vec{d} = [d_0 \, d_1 \, d_2 \, \dots \, d_6]$ and $\vec{e} = [e_0 \, e_1 \, e_2 \, \dots \, e_6]$ are polynomial parameters. $f(t) = [1 \; t \; t^2 \; t^3 \; \dots \; t^6]^T$, and $t \in [t_0, t_f]$. Denotations $x(t)$, $y(t)$ and $z(t)$ are the coordinates of flying vehicle's position. The polynomial order is specified by six such that the paths become flexible enough to satisfy collision-free criterion and optimal performance.

Recalling the flying vehicle state $q = (x, y, z, v, \psi, \gamma, \sigma)^T$, the kinematics and the motion in (2)(3), and taking the time derivatives of $\dot{x}, \dot{y}, \dot{z}$ and substituting $\dot{v}, \dot{\gamma}, \dot{\psi}$, we get the higher differential order of states as $\ddot{x}, \ddot{y}, \ddot{z}$:

$$\begin{aligned} \ddot{x} &= F_T cos\gamma cos\psi / M - F_N cos\sigma sin\gamma cos\psi / M - sin\psi F_N sin\sigma / M \\ \ddot{y} &= F_T cos\gamma sin\psi / M - F_N cos\sigma sin\gamma sin\psi / M + F_N sin\sigma cos\psi / M \\ \ddot{z} &= F_T sin\gamma / M + F_N cos\sigma cos\gamma / M - g \end{aligned} \qquad (6)$$

The reference force inputs F_T and F_N at boundary states can also be provided as prior experience. Then it is followed from (2) and (6) that the given boundary conditions can be transferred to equations related to zero, 1st and 2nd differential order of the state variables x, y, z respectively. To

that end, we can obtain the redefined boundary conditions as follows.

$$q_x = (\quad x_0 \quad x_f \quad \frac{dx}{dt}\big|_{t_0} \quad \frac{dx}{dt}\big|_{t_f} \quad \frac{d^2x}{dt^2}\big|_{t_0} \quad \frac{d^2x}{dt^2}\big|_{t_f} \quad)$$

$$q_y = (\quad y_0 \quad y_f \quad \frac{dy}{dt}\big|_{t_0} \quad \frac{dy}{dt}\big|_{t_f} \quad \frac{d^2y}{dt^2}\big|_{t_0} \quad \frac{d^2y}{dt^2}\big|_{t_f} \quad) \quad (7)$$

$$q_z = (\quad z_0 \quad z_f \quad \frac{dz}{dt}\big|_{t_0} \quad \frac{dz}{dt}\big|_{t_f} \quad \frac{d^2z}{dt^2}\big|_{t_0} \quad \frac{d^2z}{dt^2}\big|_{t_f} \quad)$$

To further address the dynamically changing environment, we assume the piecewise-constant parameterized trajectory (5), that is, within the time interval $t \in [t_0 + kT_s, t_0 + (k+1)T_s]$ $(k = 0, 1, \ldots \bar{k} - 1)$, coefficients c_i^k and d_i^k, $i = 0, \cdots, 6$ are constants, where T_s is the sampling time, and $\bar{k}$ is the maximum integer less than T/T_s. Then the parameterized trajectory for the vehicle during the kth sampling time interval can be rewritten as

$$
\begin{aligned}
x(t) &= \bar{f}(t)(G^k)^{-1}(E^k - H^k c_6^k) + c_6^k t^6 \\
y(t) &= \bar{f}(t)(G^k)^{-1}(F^k - H^k d_6^k) + d_6^k t^6 \\
z(t) &= \bar{f}(t)(G^k)^{-1}(I^k - H^k e_6^k) + e_6^k t^6
\end{aligned}
\quad (8)
$$

where $\bar{f}(t) = \begin{bmatrix} 1 & t & t^2 & t^3 & t^4 & t^5 \end{bmatrix}$, and

$$
G^k = \begin{bmatrix}
1 & t_k & t_k^2 & t_k^3 & t_k^4 & t_k^5 \\
1 & t_f & t_f^2 & t_f^3 & t_f^4 & t_f^5 \\
0 & 1 & 2t_k & 3t_k^2 & 4t_k^3 & 5t_k^4 \\
0 & 1 & 2t_f & 3t_f^2 & 4t_f^3 & 5t_f^4 \\
0 & 0 & 2 & 6t_k & 12t_k^2 & 20t_k^3 \\
0 & 0 & 2 & 6t_f & 12t_f^2 & 20t_f^3
\end{bmatrix}
$$

$$E^k = \begin{bmatrix} x_k & x_f & \frac{dx}{dt}\big|_{t_k} & \frac{dx}{dt}\big|_{t_f} & \frac{d^2x}{dt^2}\big|_{t_k} & \frac{d^2x}{dt^2}\big|_{t_f} \end{bmatrix}^T$$

$$F^k = \begin{bmatrix} y_k & y_f & \frac{dy}{dt}\big|_{t_k} & \frac{dy}{dt}\big|_{t_f} & \frac{d^2y}{dt^2}\big|_{t_k} & \frac{d^2y}{dt^2}\big|_{t_f} \end{bmatrix}^T$$

$$I^k = \begin{bmatrix} z_k & z_f & \frac{dz}{dt}\big|_{t_k} & \frac{dz}{dt}\big|_{t_f} & \frac{d^2z}{dt^2}\big|_{t_k} & \frac{d^2z}{dt^2}\big|_{t_f} \end{bmatrix}^T$$

$$H^k = \begin{bmatrix} t_k^6 & t_f^6 & 6t_k^5 & 6t_f^5 & 30t_k^4 & 30t_f^4 \end{bmatrix}^T$$

(9)

It should be noted that since t_k will not be equal to t_f, matrix G^k in (9) could avoid singularity problems. Therefore, by considering (5) derived from those redefined boundary conditions, the coefficients therein can be solved by three independent parameters c_6^k, d_6^k and e_6^k to generate a class of feasible trajectories. Once the trajectory is solved in the form of (8), the corresponding state and motion of a flying vehicle can be derived top down by the following equations.

$$v = \pm\sqrt{\dot{x}^2 + \dot{y}^2 + \dot{z}^2}, \quad \psi = atan\frac{\dot{y}}{\dot{x}}, \quad \dot{\psi} = \frac{\ddot{y}\dot{x} - \dot{y}\ddot{x}}{\dot{x}^2 + \dot{y}^2}$$

$$\gamma = atan\frac{\dot{z}cos\psi}{\dot{x}}, \quad \dot{\gamma} = \frac{\ddot{z}\dot{x}cos^3\psi - \dot{z}\ddot{x}cos\psi + \dot{z}\dot{x}\dot{\psi}sin\psi}{\dot{x}^2 + \dot{z}^2cos^2\psi}$$

$$\dot{v} = \frac{\ddot{x}cos\psi - \dot{x}\dot{\psi}sin\psi + \dot{x}cos\psi tan\gamma}{cos\gamma}$$

(10)

To guarantee that the obtained motion and control inputs are compatible, we consider the motion variables $\dot{v}, \gamma, \dot{\psi}$ in the simultaneous equations (3) and (10), from which the control

inputs such as σ, F_N, F_T can thereby be designed top down as follows.

$$\sigma = atan\frac{\frac{M\dot{x}\dot{\psi}}{cos\psi}}{\frac{M\dot{\gamma}\dot{x}}{cos\psi cos\gamma} + Mgcos\gamma}, \quad F_N = \frac{M\dot{x}\dot{\psi}}{sin\sigma cos\psi}$$

$$F_T = \frac{M(\ddot{x} + \dot{\psi}\dot{x}tan\psi)}{cos\gamma cos\psi} + M(g+1)sin\gamma + F_N sin\gamma$$

(11)

Now, the first three constraints in (4) have been addressed. The corresponding reference control inputs are also provided for the purpose of trajectory tracking. It follows from the parameterized trajectory in (8) that the rest motion planning problem boils down to solve for c_6^k, d_6^k and e_6^k based on optimality and constraints due to collision avoidance criterion.

B. Trajectory Planning with Collision Avoidance Constraints

In Fig.2, the flying vehicle's velocity and radius are represented by v and R. During one sampling period $t \in [t_0 + kT_s, t_0 + (k+1)T_s]$ (often small enough), the velocity v_i^k of the ith detected dynamic obstacle (with radius r_i) can be regarded as constant. The ellipsoid-like static obstacle (Hill) is fixed in the flat. We assume that the information of nearby obstacles (within sensing range), including their positions, shapes and motion can all be sensed by the vehicle at every sampling instant $t = t_0 + kT_s$.

During $t \in [t_0 + kT_s, t_f]$, the ith dynamic obstacles is considered to be static at the position (x_i^k, y_i^k, z_i^k), and the relative velocity of the flying vehicle to the ith obstacle is defined as $(v_{i,x}^k, v_{i,y}^k, v_{i,z}^k)$. Then the distance between center M of the vehicle and center O_i^k of the ith obstacle must be at least the minimum safety distance:

$$(x_i'(t) - x_i^k)^2 + (y_i'(t) - y_i^k)^2 + (z_i'(t) - z_i^k)^2 \geq (r_i + R)^2 \quad (12)$$

where $x_i'(t) = x(t) - v_{i,x}^k\tau$, $y_i'(t) = y(t) - v_{i,y}^k\tau$, $z_i'(t) = z(t) - v_{i,z}^k\tau$ (relative position of the flying vehicle with respect to the ith dynamic obstacle), $\tau = t - (t_0 + kT_s)$, for $t \in [t_0 + kT_s, t_f]$.

For the jth ellipsoid-like obstacle, the collision avoidance criterion can be formulated as follows.

$$z(t) - z_j^h \geq -[(x(t) - x_j^h)^2/m_j^2 + (y(t) - y_j^h)^2/n_j^2] \quad (13)$$

where (x_j^h, y_j^h, z_j^h) is the coordinate of the peak position of the jth ellipsoid-like obstacle. m_j and n_j are parameters that can be adjusted to incorporate different shapes of those static obstacles.

Now, we can substitute trajectory model (8) of the vehicle into (12) and (13) in order to create a collision free principle related to c_6^k, d_6^k, e_6^k.

For the ith dynamic obstacle, the constrained set is denoted by $\Omega_{d,i,t}^k$:

$$(c_6^k + \frac{g_{1,i}^k(t)}{g_2^k(t)})^2 + (d_6^k + \frac{g_{3,i}^k(t)}{g_2^k(t)})^2 + (e_6^k + \frac{g_{4,i}^k(t)}{g_2^k(t)})^2 \geq \frac{(r_i + r_0)^2}{(g_2^k(t))^2}$$

(14)

where

$$g_{1,i}^k(t) = \bar{f}(G^k)^{-1}E^k - v_{i,x}^k\tau - x_i^k, \quad g_2^k(t) = t^6 - \bar{f}(G^k)^{-1}H^k$$

$$g_{3,i}^k(t) = \bar{f}(G^k)^{-1}F^k - v_{i,y}^k\tau - y_i^k$$

$$g_{4,i}^k(t) = \bar{f}(G^k)^{-1}I^k - v_{i,z}^k\tau - z_i^k, \quad \bar{f} = \begin{bmatrix} 1 & t & t^2 & t^3 & t^4 & t^5 \end{bmatrix} \tag{15}$$

For the jth ellipsoid-like static obstacle, the constrained set is denoted by $\Omega_{s,j,t}^k$:

$$e_6^k \geq l_{1,j}(t)(c_6^k)^2 + l_{2,j}(t)c_6^k + l_{3,j}(t)(d_6^k)^2 + l_{4,j}d_6^k + l_{5,j}(t) \tag{16}$$

where

$$l_{1,j}(t) = -\frac{t^6 - \bar{f}(G^k)^{-1}H}{m_j^2}, \quad l_{2,j}(t) = -\frac{2(\bar{f}(G^k)^{-1}E^k - x_j^h)}{m_j^2}$$

$$l_{3,j}(t) = -\frac{t^6 - \bar{f}(G^k)^{-1}H}{n_j^2}, \quad l_{4,j}(t) = -\frac{2(\bar{f}(G^k)^{-1}F^k - y_j^h)}{n_j^2}$$

$$l_{5,j}(t) = -\frac{(\bar{f}(G^k)^{-1}E^k - x_j^h)^2}{m_j^2(t^6 - \bar{f}(G^k)^{-1}H^k)} - \frac{\bar{f}(G^k)^{-1}I^k - z_j^h}{t^6 - \bar{f}(G^k)^{-1}H^k}$$
$$- \frac{(\bar{f}(G^k)^{-1}F^k - y_j^h)^2}{n_j^2(t^6 - \bar{f}(G^k)^{-1}H^k)} \tag{17}$$

The constrained domain of c_6^k, d_6^k and e_6^k due to collision avoidance criterion are obtained from (14) and (16). Considering all the detected obstacles, we could obtain the general constrained domain Ω_d^k and Ω_s^k as follows.

$$\begin{cases} \Omega_d^k = \bigcap_{i=1}^{i_k} \Omega_{d,i,t}^k, & t \in \left[t_0 + kT_s, t_f\right] \\ \Omega_s^k = \bigcap_{j=1}^{j_k} \Omega_{s,j,t}^k, & t \in \left[t_0 + kT_s, t_f\right] \end{cases} \tag{18}$$

where i_k and j_k are the total number of detected dynamic and terrain static obstacles at sampling instant $t = t_k$ respectively.

C. Optimal Solution and Solvability of Candidate Trajectories

To evaluate the arc length of the generated trajectory, the integral of quadratic form of thrusting velocity $|v|$ with respect to time can be employed as the PI for the paths:

$$J_k(c_6^k, d_6^k, e_6^k) = \int_{t_k}^{t_f} v^2 dt = \int_{t_k}^{t_f}(\dot{x}^2 + \dot{y}^2 + \dot{z}^2)dt \tag{19}$$

To this end, the optimization problem related to shortest trajectory generation becomes

$$\min J_k(c_6^k, d_6^k, e_6^k) \tag{20}$$

The optimal solution is derived by the following Theorem.

Theorem 1: At each time instant $t_k = t_0 + kT_s$, the optimization problem (20) is always solvable, and its solutions are

$$c_6^{k*} = -s_1^k/(2s_2^k), \quad d_6^{k*} = -s_4^k/(2s_2^k), \quad e_6^{k*} = -s_5^k/(2s_2^k) \tag{21}$$

where s_1^k, s_2^k, s_4^k and s_6^k are given in equations (23).

Proof: Since $\dot{x}$, $\dot{y}$ and $\dot{z}$ are also polynomials in terms of t and coefficients c_6^k, d_6^k and e_6^k, then the PI can be rewritten as

$$J_k(c_6^k, d_6^k, e_6^k) = \int_{t_k}^{t_f}(\dot{x}^2 + \dot{y}^2 + \dot{z}^2)dt$$
$$= s_2^k(c_6^k + \frac{s_1^k}{2s_2^k})^2 + s_2^k(d_6^k + \frac{s_4^k}{2s_2^k})^2 + s_2^k(e_6^k + \frac{s_5^k}{2s_2^k})^2$$

$$+ (s_0^k + s_3^k + s_6^k) - [(s_1^k)^2 + (s_4^k)^2 + (s_5^k)^2]/(4s_2^k) \tag{22}$$

where

$$s_0^k = \int_{t_k}^{t_f}(\bar{f}'(G^k)^{-1}E^k)^2 dt, \quad s_6^k = \int_{t_k}^{t_f}(\bar{f}'(G^k)^{-1}I^k)^2 dt$$

$$s_1^k = 2\int_{t_k}^{t_f}(6t^5 - \bar{f}'(G^k)^{-1}H^k)(\bar{f}'(G^k)^{-1}E^k)dt$$

$$s_2^k = \int_{t_k}^{t_f}(6t^5 - \bar{f}'(G^k)^{-1}H^k)^2 dt, \quad s_3^k = \int_{t_k}^{t_f}(\bar{f}'(G^k)^{-1}F^k)^2 dt$$

$$s_4^k = 2\int_{t_k}^{t_f}(6t^5 - \bar{f}'(G^k)^{-1}H^k)(\bar{f}'(G^k)^{-1}F^k)dt$$

$$s_5^k = 2\int_{t_k}^{t_f}(6t^5 - \bar{f}'(G^k)^{-1}H^k)(\bar{f}'(G^k)^{-1}I^k)dt$$

$$\bar{f}' = \begin{bmatrix} 0 & 1 & 2t & 3t^2 & 4t^3 & 5t^4 \end{bmatrix} \tag{23}$$

Since the integration terms of $s_0^k \sim s_6^k$ are constant at each sampling instant, it follows from the last equation in (22) that J_k is minimized if the solution in (21) are applied. This completes the proof. $\square$

If we consider the optimal solution (21) in a 3D parameter space of $c_6 - d_6 - e_6$, it becomes one fixed point O^{k*} with coordinates $(c_6^{k*}, d_6^{k*}, e_6^{k*})$. Recalling the last equation in (22), it can be found that the contour of the PI is a series of spheres centered at (21). To that end, recalling the original problem (4) and the constrained domain in (18) governed by collision avoidance criterion, we can reformulate the optimization problem in the $c_6 - d_6 - e_6$ parameter space as follows:

$$\min \, dis\{O^k, O^{k*}\}, \quad s.t. \, O^k \in \Omega_d^k \cap \Omega_s^k \tag{24}$$

where the coordinates of O^k denote the candidate solutions of the three parameters. Such an optimization problem can be well solved in the $c_6 - d_6 - e_6$ parameter space by specifying the position of O^k so that it stays as close to the optimal point O^{k*}, while located in the intersection regions of constraints sets Ω_d^k (exterior region of a sets of spheres) and Ω_s^k (exterior region of a sets of elliptic paraboloid). Generally, the solution process is as follows:

- If $O^{k*} \in \Omega_d^k \cap \Omega_s^k$, then the trajectory can be directly specified by $(c_6^{k*}, d_6^{k*}, e_6^{k*})$ $(O^k = O^{k*})$.
- If $O^{k*} \notin \Omega_d^k \cap \Omega_s^k$, then we have to incrementally expand the PI contour in order to search for an alternative feasible suboptimal solution. In such case, the suboptimal solution point $O^{k*'}(c_6^{k*'}, d_6^{k*'}, e_6^{k*'})$ can be found as follows.

$$c_6^{k*'} = c_6^{k*} + \sqrt{\frac{i\lambda}{s_2^k}}\sin\alpha\cos\beta, \quad d_6^{k*'} = d_6^{k*} + \sqrt{\frac{i\lambda}{s_2^k}}\sin\alpha\sin\beta$$

$$e_6^{k*'} = e_6^{k*} + \sqrt{\frac{i\lambda}{s_2^k}}\cos\alpha \tag{25}$$

where λ denotes the length of each search step along the radius vector of the sphere PI contour, and the number of steps is denoted by i ($i = 0, 1, 2, \ldots$). $\alpha, \beta \in [0 \; 2\pi)$

are two angle parameters that determine the searching density on each sphere contour, e.g. they may be formulated as $\alpha, \beta = \frac{j\pi}{180}, j = 0, 1, \ldots, 359$. After completing each searching step, the optimal point O^{k*} is replaced by candidate suboptimal point $O^{k*'}$ and then checked by the first condition until the desired suboptimal solution is found.

On the other hand, if no feasible solutions are found within the maximum number of searching steps due to the highly cluttered environment, the maneuver time T should be prolonged such that the vehicle can run a bigger smooth detour with slower speed to pass through the obstacles.

In real-world application, the intersection regions can be handled by their projections on the three 2-D planes respectively so that it is easier to compute the analytic solutions. For example, when considering one dynamic obstacle and one static hill-like obstacle, we can obtain the constrained area projected on the $c_6 - e_6$ plane similar as that illustrated in Fig.3.
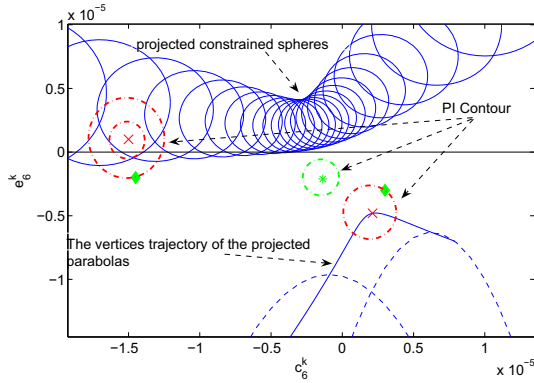
Fig. 3.   Projections of optimal/suboptimal points, constraint spheres Ω_d^k, the vertices trajectories and the horizon boundary of the projected constraint elliptic paraboloids Ω_s^k on $c_6 - e_6$ plane.

Two kinds of solution situations are shown in the 2D parameter space. The green star optimal point is located in the 'safe' area outside the region of both projected constraint sphere areas and elliptic paraboloid areas, thereby O^k can be directly specified by $= (c_6^{k*}, d_6^{k*}, e_6^{k*})$ in (24). If optimal point O^{k*} is located outside the constrained domain as the two red fork points, then the PI contour needs to be expanded until a feasible suboptimal point is found, as the two green diamond points show. In this case, the candidate suboptimal solution should be valued by $O^k = (c_6^{k*'}, d_6^{k*'}, e_6^{k*'})$. Generally, after projecting the intersection areas on the three corresponding planes, based on optimal index in (24), one can choose the most desired suboptimal solution according to the distance between the three candidate suboptimal points and the optimal point from respective planes. If only the feasible trajectory exists, we can always compute the desired optimal or suboptimal path based on the proposed approach.

IV. SIMULATION

First, we consider the situation that the vehicle flies through multiple static obstacles (hills). Our approach is compared with another similar parametric method. In this section, the scales are the same. All quantities conform to a given unit system. The information of static obstacles are shown in Table I, and the task settings are as follows:

- Flying vehicle settings: $R=2$, $M = 1.5 * 10^4$, $g=9.8$.
- Boundary Conditions: $q^0 = \left(10, 10, 0, 1, \frac{\pi}{6}, \frac{\pi}{4}, \frac{\pi}{850}\right)$ and $q^f = \left(90, 90, 0, 2, \frac{\pi}{10}, \frac{\pi}{5}, -\frac{\pi}{850}\right)$.
- Maneuver time: $t_0=0$, $t_f=40$s.
- Sampling time interval: Ts=1s.

TABLE I
SETTINGS OF THE STATIC OBSTACLES

obstacle	x_j	y_j	z_j	m_j	n_j
1	20	30	20	4	2
2	60	20	25	2	2.5
3	40	60	20	5	4
4	90	60	10	4	3
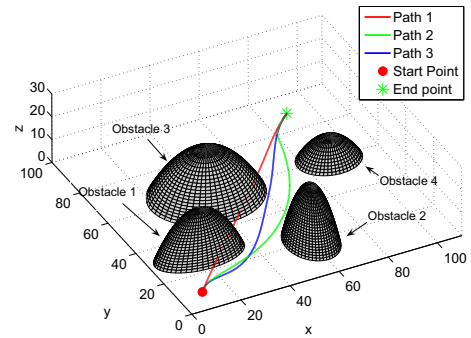
Fig. 4.   The trajectories comparison of flying vehicle among static obstacles (hills).

In Fig.4, a flying vehicle is expected to move safely from initial position to final position. There are three trajectories generated by our optimal and suboptimal solutions (path 1 and path 3), and by a similar work (path 2) in [10] respectively. Path 1 is rendered with the optimal solution in (21), and it collides with obstacle 1 and 3 since it does not consider the obstacles. Path 2 is computed by a similar parametric trajectory model with a lower order, which potentially weakens the optimal performance. A more desirable collision-free Path 3 with shorter path length is generated with the suboptimal solution in (25). In fact, after fitting different trajectory model, the redefined optimal problem in (24) can also be exploited to assess the optimality of analytic solutions such as [10][11] as well.

To consider the validity of our suboptimal approach in dynamic unknown environment, two movable obstacles are added to create a cluttered environment. The boundary conditions are updated by $q^0 = \left(10, 10, 0, 1, \frac{\pi}{6}, \frac{\pi}{4}, \frac{\pi}{850}\right)$ and $q^f = \left(100, 80, 30, 2, \frac{\pi}{10}, \frac{\pi}{5}, -\frac{\pi}{850}\right)$. The information of two dynamic obstacles are shown in Table II and the rest settings are identical to those in the previous example. The radius of the movable obstacles are $r_1 = r_2 = 2$.

In Fig.5, a vehicle is flying through the cluttered 3D environment containing two moving obstacles and four static

TABLE II
SETTINGS OF THE DYNAMIC OBSTACLES

obs.	pos.	$v_i^0 (t \in [0,10])$	$v_i^1 (t \in (10,20])$	$v_i^2 (t \in (20,40])$
1	(45,0,5)	$(0,2.5,0)^T$	$(0,1,1)^T$	$(0.2,-0.2,0)^T$
2	(77,74,21)	$(0,-0.2,0)^T$	$(0,-0.2,0)^T$	$(0.2,0.7,-0.7)^T$
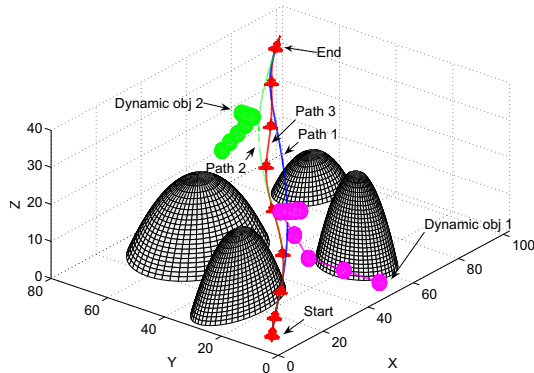
Fig. 5. The trajectories for the flying vehicle in 3D cluttered environment.
.

hills. The vehicle (red) and two movable obstacles (magenta and green) that are marked by spheres are drawn every 5 seconds. According to the detected obstacle information within $0 \sim 10s$, the initial blue path 1 is computed by our suboptimal solution in order to avoid collision with the static obstacle 1 and the dynamic obstacle 1. However, such a path could still collide with dynamic obstacle 1 at 18s whose motion changes at 10s. When the vehicle detects this information at 10s, the rest path is adjusted instantly by green path 2 to successfully get rid of dynamic obstacle 1. Likewise, when the motion of dynamic obstacle 2 changes and is detected at 20s, the vehicle replans its path by red path 3 to keep away from potential collision that exists in path 2 within $28 \sim 32s$. Governed by the rule of suboptimality, the red path 3 rapidly converges to the optimal one after the vehicle passes the obstacles. Value of three parameters that determine these three trajectories are ($\times 10^{-7}$)

$$\begin{cases} c_6^1 = -0.2 \\ d_6^1 = 1 \\ e_6^1 = -0.25 \end{cases}, \begin{cases} c_6^2 = 5.13 \\ d_6^2 = -1 \\ e_6^2 = 0.29 \end{cases}, \begin{cases} c_6^3 = 36.01 \\ d_6^3 = 63.97 \\ e_6^3 = -2.87 \end{cases}$$

The corresponding yaw-pitch-roll angles and input forces of the flying vehicle along path 3 are shown in Fig.6, all of
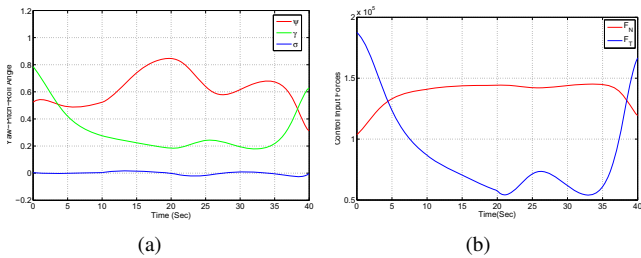
Fig. 6. The angles and controls of the flying vehicle. (a) The trajectory of the vehicle Euler angles. (b) The trajectory of two resultant input forces.

which are stable and smooth. Different from other methods such as [10][11], the trajectories of motion and controls derived by our approach are always second order differentiable and continuous since higher order state variables $\dddot{x}, \dddot{y}, \dddot{z}$ are considered, thereby making the method valid for real-world applications.

V. CONCLUSIONS

This paper presents an analytical solution to design an online motion planner for a fixed wing vehicle in 3D dynamic space. The proposed method employs piecewise parameterized polynomials to construct the optimal trajectory, taking into consideration of kinematics and geometric constraints due to obstacles. A novel 3D parameter space is developed to unify the discussion of the reformulated constraints and the solution to the optimization problem. Such a constrained optimization problem can thereby be solved based on its geometric significance in that space. Compared to other parametric approaches, the resultant control inputs are always continuous and the performance of the trajectories are better improved. The simulation results verify the effectiveness of our method. Such a method could also be exploited for local trajectory optimization in search-based methods.

VI. ACKNOWLEDGMENT

REFERENCES

[1] S. M. LaValle, *Planning algorithms*. Cambridge Univ Press, 2006.
[2] N. X. Vinh, *Flight mechanics of high-performance aircraft*. Cambridge Univ Press, 1995, vol. 4.
[3] S. M. LaValle and J. J. Kuffner, "Randomized kinodynamic planning," *Int. J. Robot. Res.*, vol. 20, no. 5, pp. 378–400, 2001.
[4] S. Karaman and E. Frazzoli, "Sampling-based algorithms for optimal motion planning," *Int. J. Robot. Res.*, vol. 30, no. 7, pp. 846–894, 2011.
[5] D. G. Macharet, A. A. Neto, and M. Campos, "On the generation of feasible paths for aerial robots in environments with obstacles," in *Proc. IEEE Int. Conf. Intell. Robots Syst.*, 2009, pp. 3380–3385.
[6] P.-Y. Wu, D. Campbell, and T. Merz, "Multi-objective four-dimensional vehicle motion planning in large dynamic environments," *IEEE Trans. Syst., Man, Cybern. B, Cybern.*, vol. 41, no. 3, pp. 621–634, 2011.
[7] Z. Qu, J. Wang, and C. E. Plaisted, "A new analytical solution to mobile robot trajectory generation in the presence of moving obstacles," *IEEE Trans. Robot.*, vol. 20, no. 6, pp. 978–993, 2004.
[8] H. Yuan and T. Shim, "Model based real-time collision-free motion planning for nonholonomic mobile robots in unknown dynamic environments," *Int. J. Precis. Eng. Man.*, vol. 14, no. 3, pp. 359–365, 2013.
[9] J. Yang, Z. Qu, J. Wang, and K. Conrad, "Comparison of optimal solutions to real-time path planning for a mobile vehicle," *IEEE Trans. Syst., Man, Cybern. A, Syst., Humans*, vol. 40, no. 4, pp. 721–731, 2010.
[10] H. Yuan and Z. Qu, "Optimal real-time collision-free motion planning for autonomous underwater vehicles in a 3d underwater space," *IET. Control. Theory. A.*, vol. 3, no. 6, pp. 712–721, 2009.
[11] J. Yang, Z. Qu, J. Wang, and R. A. Hull, "Real-time optimized trajectory planning for a fixed-wing vehicle flying in a dynamic environment," *J. Aerospace. Eng.*, vol. 22, no. 4, pp. 331–341, 2009.